analytical chemistry

pubs.acs.org/ac Article

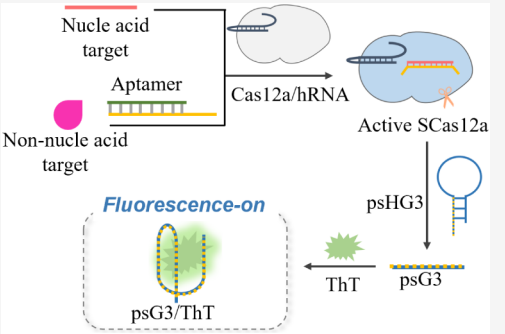
Phosphorothioate-Modified Hairpin G-Triplex Reporter-Assisted Split CRISPR/Cas12a-Powered Biosensor for "Turn-On" Fluorescent Detection of Nucleic Acid and Non-Nucleic Acid Targets

Kai Shi,* Wenjie Luo, Ying Cheng, Honglei Li, Liai Peng, Xiangrui Luo, Yu Hu,* Jiaheng Zhang,* and Jiaxuan Chen*

Cite This: https://doi.org/10.1021/acs.analchem.5c00140 Read Online

ACCESS | Metrics & More | Article Recommendations | Supporting Information

ABSTRACT: CRISPR/Cas12a-powered biosensors with guanine (G)-rich sequence reporters (e.g., G-quadruplex and G-triplex) are widely used in detection applications due to their simplicity and sensitivity. However, when these biosensors are employed for molecular detection in complex samples, they may encounter difficulties such as high background signal and susceptibility to interference because of the "turn-off" signal output. Herein, we explore, for the first time, a set of phosphorothioate (ps)-modified G-quadruplex (G4) and G-triplex (G3) sequences that can bind with thioflavin T (ThT) in an active split CRISPR/Cas12a system (SCas12a) to generate a "turn-on" fluorescent signal. To apply this new phenomenon, we develop a universal SCas12a-powered biosensor for "turn-on" fluorescent detection of nucleic acid (miRNA-21) and non-nucleic acid (kanamycin) targets by using ps-modified hairpin G3 as a reporter (SCas12a/psHG3). Target recognition activates SCas12a's *trans*-cleavage activity, leading to cleavage at the loop region of the psHG3 reporter. The released prelocked psG3 DNA binds ThT to produce a strong fluorescence signal. Without preamplification, this strategy can detect miRNA-21 with a detection limit of 100 fM. Moreover, the SCas12a/psHG3 system was further utilized for detecting kanamycin by incorporating its aptamers, enabling the detection of kanamycin at concentrations as low as 100 pM. This work is the first to develop a "turn-on" SCas12a/psHG3 system, showcasing its improved performance and wide range of applications in synthetic biology-based sensing technology.



The molecular detection of nucleic acids and non-nucleic acids is vital for diagnosing diseases, monitoring the environment, and ensuring food safety.[1−4] However, due to the low abundance, easy degradation, and susceptibility to interference from the detection environment of the target molecules in the test sample, it is difficult to effectively detect and quantify them.[5−7] This aforementioned challenge has hindered the development of simple, sensitive, and specific detection methods that have the potential to revolutionize molecular detection. Currently, the polymerase chain reaction (PCR) is the gold standard method for detecting nucleic acid targets, while methods for detecting non-nucleic acid targets (such as metal ions, viruses, and small molecules) include enzyme-linked immunosorbent assay (ELISA), high-performance liquid chromatography (HPLC), and mass spectrometry (MS), among others.[8−13] Unfortunately, these methods are costly to detect, are time-consuming, and require strict experimental conditions, making them difficult to apply in resource-limited scenarios. There is a pressing need for a straightforward, affordable, and resilient biological sensing platform that can handle complex environmental disruptions.

CRISPR/Cas technology is an innovative gene-editing tool that enables precise modification of genome sequences for research on gene function, treatment of genetic diseases, and other related applications.[14,15] CRISPR/Cas has been modified for biosensing applications since 2017, demonstrating its impressive ability to recognize and cleave nucleic acids.[16] Among the CRISPR/Cas family, CRISPR/Cas12a is widely used due to its ability to recognize specific single-stranded DNA (ssDNA) or double-stranded DNA (dsDNA) by guide RNA (gRNA) and subsequently activate its *trans*-cleavage activity.[17,18] Utilizing gRNA-programmed *trans*-cleavage activity is common in developing novel biosensors for detecting nucleic acid and non-nucleic acid targets.[19−21] In comparison to the direct detection of DNA, RNA targets need to undergo reverse transcription to be converted into DNA before they can be detected by Cas12a. Detecting miRNA, a short RNA of about 19−23 nucleotides, presents additional challenges in

Received: January 8, 2025
Revised: April 15, 2025
Accepted: April 17, 2025

Downloaded via SHANGHAI NORMAL UNIV on April 24, 2025 at 13:56:36 (UTC).
See https://pubs.acs.org/sharingguidelines for options on how to legitimately share published articles.

© XXXX American Chemical Society

obtaining high-quality DNA through reverse transcription. Recently, Qiao and Xiong have reported that splitting gRNA (guide RNA) into handle RNA (hRNA) and spacer RNA (sRNA) in the CRISPR/Cas12a system still retains *trans*-cleavage activity (called SCas12a).[22,23] This allows for the replacement of sRNA with target RNA to achieve direct detection of RNA. Compared to the traditional Cas12a system, the SCas12a system is capable of detecting nucleic acid targets at the femtomolar level without preamplification. However, the application of the SCas12a system to the detection of non-nucleic acid targets remains to be explored. Additionally, the signal output of the developed biosensors uses active Cas12a or SCas12a to cleave the reporter probe, which is an ssDNA molecule functionalized with a signal fragment. The reporter splitting causes the signal molecules to separate, leading to diverse signal outputs, including fluorescence, electrochemical, colorimetric, etc.[24−26] Among these methods, fluorescence is not only convenient but also effective, sensitive, and accurate, making it a promising option for detecting target biomarkers. However, the traditional fluorescence reporter for Cas12a or SCas12a commonly involves ssDNA labeled with a fluorophore (F) and a quencher (Q), thereby increasing the detection cost.[27,28]

Guanine-rich (G-rich) DNA sequences (e.g., G-quadruplex and G-triplex) can fold into four- and three-stranded noncanonical secondary structures (termed G4 and G3, respectively) through Hoogsteen-like hydrogen bonds. Research has reported that G4 and G3 can bind thioflavin T (ThT) to exhibit strong fluorescence.[29,30] Based on this, G4 and G3 have been widely used as fluorescence reporters in the CRISPR/Cas12a system. For example, Zou et al. developed a CRISPR/Cas12a-powered fluorescent biosensor for Hg^{2+} detection by using the G4-ThT complex as a reporter.[31] Liu et al. have reported that active Cas12a can rapidly cut G3 and have developed a novel biosensor by coupling Cas12a with G3 as a fluorescent reporter.[32] This tool is valuable in various fields, such as biomedical research and diagnostics, due to its ability to detect nucleic acids and non-nucleic acids with high sensitivity and specificity. However, due to the effective cleavage of G3 or G4 by active Cas12a, these "turn-off" output biosensors are prone to environmental interference and high background signals during detection.[33−35] Recently, our group has reported that phosphorothioate (ps)-modified G4 sequences can serve as a "turn-on" colorimetric/photothermal reporter for the CRISPR/Cas12a system.[36] Further research is needed to determine the effectiveness of psG-rich sequences as fluorescent signal reporters for the SCas12a system.

In this work, ps-modified G4 or G3 sequences have been systematically explored and found to be both tolerant to CRISPR/Cas12a's DNase activity and capable of binding to ThT in this system, resulting in fluorescence signals. Based on these interesting discoveries, we, for the first time, designed a novel "turn-on" fluorescent probe by using the psG3 hairpin structure (psHG3) and developed a universal SCas12a/psHG3 system for nucleic acid and non-nucleic acid target detection. To demonstrate its capabilities, miRNA-21 and kanamycin were used as models to assess the platform's detection performance. Unlike traditional FQ-labeled or G-rich reporters incorporated in CRISPR/Cas12a biosensing, the SCas12a/psHG3 system is cost-effective and "turn-on" based, utilizing the psHG3 probe, which is introduced here for the first time. This research is expected to expand the use of Cas12a-powered technologies and could potentially transform the way biomolecular markers are detected by using fluorescence.

EXPERIMENTAL SECTION

Reagents and Materials. Tetracycline, kanamycin, oxytetracycline, ciprofloxacin, ofloxacin, and sulfamerazine were purchased from Aladdin (Shanghai, China). Both Cas12a and NEBuffer 2.1 were purchased from New England Biolabs Ltd. (Beijing, China). SYBR Green I was obtained from Solarbio (Beijing, China). All the oligonucleotides (Table S1) were synthesized by Sangon Biotech (Shanghai, China).

Preparation of the psHG3 Reporter Probe. The synthesized psHG3 sequence was dissolved at a concentration of 100 μM in 20 mM Tris-HCl buffer (pH 7.4, 100 mM NaCl). The dissolved psHG3 sequence was heated at 95 °C for 5 min and then cooled to 25 °C to obtain the psHG3 reporter probe.

miRNA-21 Detection. For the miRNA-21 assay, 10 μL of various concentrations of miRNA-21 were mixed with 40 μL of a solution containing 125 nM Cas12a, 125 nM hRNA, 125 nM ssDNA activator, 1.25x NEBuffer 2.1, 2.5 μM ThT, and 2.5 μM psHG3 probe at 37 °C for 30 min. To test the selectivity of the SCas12a/psHG3 system, 20 pM miRNA-21 and 200 pM of other interfering miRNAs (miRNA-17, miRNA-155, miRNA-141, and miRNA-10b) were employed, respectively. To explore the applicability of the SCas12a/psHG3 system in serum samples, three different concentrations of miRNA-21 (5, 15, and 20 pM) were mixed into 10-fold-diluted human serum for testing according to the standard spiking method. The spiked human serum samples were directly analyzed without any further sample preparation.

Detection of Kanamycin. First, various concentrations of kanamycin were added to the aptamer (AP)/CP complex (100 nM) at 37 °C for 30 min to release the CP sequence. Then, 10 μL of the above reaction solution was added to 40 μL of the mixture solution containing 125 nM Cas12a, 125 nM hRNA, 125 nM sRNA, 1.25× NEBuffer 2.1, 2.5 μM ThT, and 2.5 μM psHG3 probe. Finally, incubation at 37 °C for 30 min was performed to activate the *trans*-cleavage activity of SCas12a, followed by the formation of the psHG3/ThT complex to obtain the fluorescence signal. To evaluate the selectivity of the SCas12a/psHG3 system, 30 nM kanamycin and 3 μM of other nontarget antibiotics were used as replacements . To explore the applicability of the SCas12a/psHG3 system in environmental water samples, three different concentrations of kanamycin (5, 18, and 30 nM) were incubated with laboratory tap water and river water (Leshan, China), respectively. Filter papers were employed to filter out insoluble impurities from the river samples. The aforementioned procedures were executed in a manner identical to those detailed previously.

Fluorescence Measurement and Melting Curve Procedures. The fluorescence of the sample solution was measured from 450 to 600 nm by using a Lengguang F98 fluorescence spectrophotometer (Shanghai Lengguang Technology Co., Ltd., China), with the excitation fixed at 430 nm. The fluorescence intensity was measured at a wavelength of 490 nm.

The Tm values of the hairpin psHG3 reporter probe incubated with or without activated SCas12a were evaluated by conducting melting curve experiments. The 20 μL reaction mixture contained 1× NEBuffer 2.1, 100 nM psHG3 reporter, and 10× SYBR Green. All reaction mixtures were placed in a

https://doi.org/10.1021/acs.analchem.5c00140
Anal. Chem. XXXX, XXX, XXX−XXX

real-time fluorescence quantitative PCR instrument (7500, ThermoFisher) for testing.

RESULTS AND DISCUSSION

The psG-Rich/ThT Complexes Show a Fluorescent Signal in the Active SCas12a System. To examine whether the ps-modified G4/ThT complex could induce fluorescence in the active SCas12a system, parallel (ps-pw17), antiparallel (ps-ps2.m), and mixed parallel/antiparallel (ps-h-telo) G4 sequences were first tested. As shown in Figure 1B, all of the

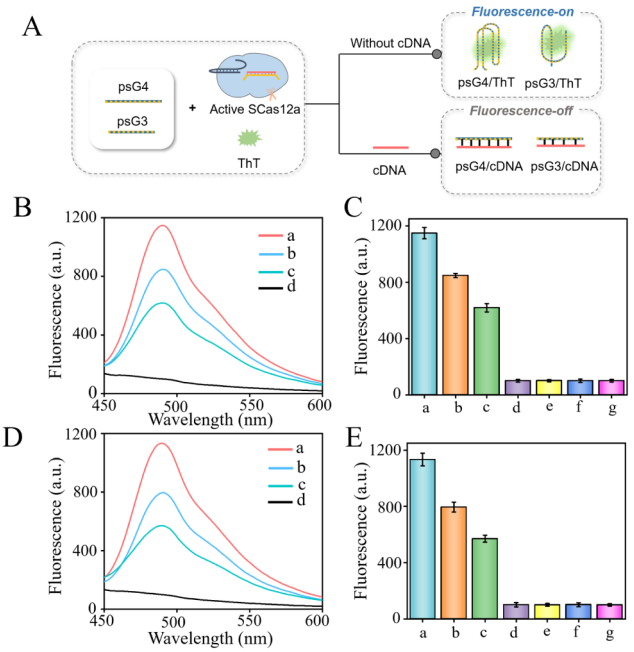


Figure 1. Fluorescence signal emitted by the psG-rich/ThT complexes in the active SCas12a system, which can be blocked by complementary DNA. (A) Schematic diagram of the binding of psG4/G3 to ThT, resulting in fluorescence emission in the active SCas12a solution, and inhibition of fluorescence output by complementary DNA. (B) Fluorescence spectra of ps-h-telo/ThT (a), ps-pw17/ThT (b), ps-ps2.m/ThT (c), and blank (d). (C) Inhibition of the fluorescence intensity of psG4/ThT by complementary DNA. ps-h-telo/ThT (a), ps-pw17/ThT (b), ps-ps2.m/ThT (c), ps-h-telo/cDNA/ThT (d), ps-pw17/cDNA/ThT (e), ps-ps2.m/cDNA/ThT (f), and blank (g). (D) Fluorescence spectra of psG3/ThT (a), psG31/ThT (b), psTBA-G3/ThT (c), and blank (d). (E) Inhibition of the fluorescence intensity of psG3/ThT by complementary DNA. ps-G3/ThT (a), ps-G31/ThT (b), ps-TBA1-G3/ThT (c), ps-G3/cDNA/ThT (d), ps-G31/cDNA/ThT (e), ps-TBA-G3/cDNA/ThT (f), and blank (g). Error bars: SD, n = 3.

ps-modified G4/ThT complexes generated a significantly higher fluorescence signal compared to the ps-modified G4-free sample. Notably, the ps-h-telo sequence produced the strongest fluorescence signal in comparison to the ps-pw17 and ps-ps2.m sequences. Once these ps-modified G4 sequences hybridized with their corresponding fully complementary DNA, the solution of active SCas12a and ThT displayed negligible fluorescence signals (Figure 1C). Next, to explore whether the ps-modified G3/ThT complex could induce fluorescence in the active SCas12a system, we mixed ThT with three types of topologies in ps-modified G3, e.g., ps-G3, ps-G31, and ps-TBA-G3, respectively. As shown in Figure 1D, the strongest fluorescence signal was obtained by ps-G3 when compared with ps-G31 and ps-TBA-G3. Similarly, the solution of active SCas12a and ThT displayed significant fluorescence signals after the above ps-G3 sequences hybridized with their corresponding fully complementary DNA (Figure 1E). Together, the above-mentioned results demonstrate that ps-G3 has the potential to serve as a "turn-on" fluorescence signal probe in the active SCas12a system.

Construction of the psHG3 Reporter Probe. Constructing the psG3/SCas12a system hinges on the development of an effective presilenced psG3 probe that could act as a versatile "turn-on" reporter probe for SCas12a's *trans*-cleavage activity. The effective silencing of psG3 before *trans*-cleavage to minimize background and the effective release of psG3 after *trans*-cleavage were two key points in the design of the reporter probe. Inspired by the previously reported G3-based hairpin reporter probe, we hypothesized that incorporating the psG3 sequence into a hairpin probe (psHG3) could serve as an effective "turn-on" reporter for the SCas12a system. The designed psHG3 reporter probe consists of two fragments: a loop region designed to be cut by active SCas12a and a ps-modified G3-forming sequence locked in the hairpin stem (Figure 2A). Figure 2B shows that the designed psHG3

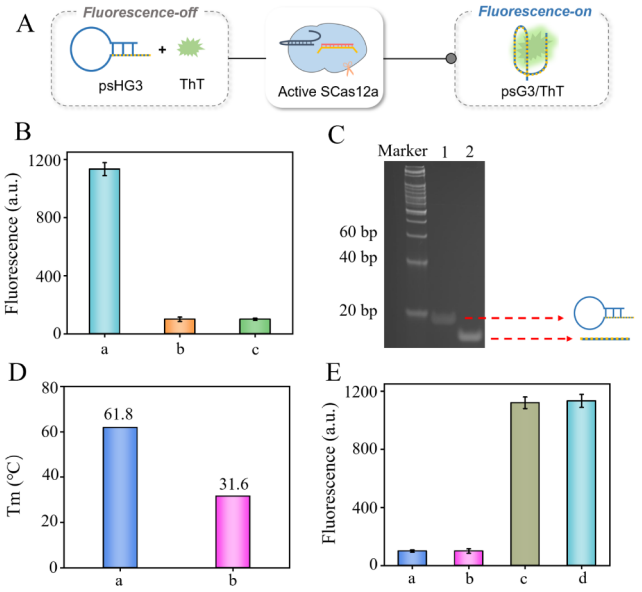


Figure 2. Design of a "turn-on" reporter probe using the psG3 sequence in the active Scas12a system. (A) The designed psHG3 functions as a fluorescence "turn-on" reporter for a SCas12a-powered biosensor. (B) Fluorescence intensity of psG3/ThT and psHG3/ThT. (a) ps-G3, (b) psHG3, and (c) blank. (C) PAGE analysis of the cleavage of psHG3 probe by active SCas12a. (D) Temperature melting values of psHG3 probe after incubation with inactive SCas12a (a) and active SCas12a (b). (E) Fluorescence intensity of the released psG3 from psHG3 probe. (a) Blank, (b) psHG3, (c) psHG3 + active SCas12a, and (d) psG3. Error bars: SD, n = 3.

reporter probe not only maintained stability but also caused a low background signal (column b). The results suggest that the psG3 sequence in the designed psHG3 reporter probe was successfully silenced. Figure 2C (lane 2) shows that the ps-modified G3-forming sequence could be released from the psHG3 probe after *trans*-cleavage by active SCas12a. We explored the Tm values of the psHG3 probe before and after being cut by active SCas12a. As shown in Figure 2D (column a) and Figure S1, the psHG3 probe remained stable at the

https://doi.org/10.1021/acs.analchem.5c00140
Anal. Chem. XXXX, XXX, XXX−XXX

reaction temperature (61.8 °C > 37 °C) in the absence of active SCas12a. As shown in Figure 2D (column b) and Figure S2, when the psHG3 probe was cleaved by active SCas12a, it caused a significant decrease in the Tm value (31.6 °C < 37 °C), explaining the release of the psG3 sequence from the psHG3 probe. Following that, we assessed the function of the released psG3 sequence from the psHG3 probe to produce a fluorescence signal. A sharp increase in the fluorescence signal was obtained, indicating that the released psG3 sequence could bind with ThT to form a psG3/ThT complex (Figure 2E). Together, the above-mentioned results demonstrate that the SCas12a/psG3 system has been successfully constructed by using the designed psHG3 as a "turn-on" reporter probe in the SCas12a strategy.

Subsequently, several experimental conditions in the SCas12a/psHG3 system were investigated, including the length of the loop and stem in the psHG3 reporter, the concentrations of the psHG3 reporter and Cas12a, and the *trans*-cleavage time of SCas12a. From Figures S3-S7, the optimal detection conditions for the SCas12a/psHG3 system were determined to be 2 μM psHG3 reporter with a 15-nt loop and a 9-nt stem, 100 nM Cas12a protein, and 30 min for the *trans*-cleavage of SCas12a.

Sensing Performance of the SCas12a/psHG3 System for miRNA-21. To demonstrate the detection performance of the SCas12a/psHG3 system under optimum conditions, miRNA-21, known for its expression dysregulation closely related to various cancers, was chosen as a model nucleic acid target.[37−40] Accurate detection of miRNA-21 is of great significance in the clinical diagnosis and treatment of related cancers. To achieve direct detection of the target miRNA-21, we designed miRNA-21 as a spacer RNA in the SCas12a system (Figure 3A). Upon the addition of miRNA-21, it complemented the ssDNA activator and activated SCas12a. The active SCas12a cleaved the hairpin DNA loop of the psHG3 reporter DNA, releasing the ps-G3 forming sequence, which then bound with ThT and provided a fluorescent signal. However, SCas12a was not activated, and psHG3 remained stable when no miRNA-21 was added, thus exhibiting low fluorescence intensity. Figure 3B shows that the signal response activated by miRNA-21 was notably higher than that of the blank control, demonstrating the feasibility of the SCas12a/psHG3 system. The sensitivity of the SCas12a/psHG3 system was evaluated over a range of miRNA-21 concentrations, including 0, 0.2, 5, 9, 12, 15, 18, and 20 pM. Figure 3C shows that the fluorescence signal augmented significantly with the increase in miRNA-21. The correlation equation is F = 56.90C + 239.78 in the range from 0.2 to 20 nM (Figure 3D, R^2 = 0.995). The limit of detection (LOD) was estimated to be 100 fM, calculated by employing the $3\sigma/K$ method (where K represents the slope of the calibration curve and σ is the standard deviation of the 11 target-free tests). The selectivity of the SCas12a/psHG3 system was verified by employing highly homologous multiple miRNAs (miRNA-17, miRNA-155, miRNA-141, and miRNA-10b). Figure 3E shows that the SCas12a/psHG3 system was insensitive to interfering miRNAs but strongly responded to miRNA-21, demonstrating that this strategy possessed preeminent selectivity. To evaluate the practical application value of the SCas12a/psHG3 system, three different concentrations of miRNA-21 (5, 15, and 20 pM) were added to diluted human serum (10%) for the recovery experiment. Results, as shown in Table S2, indicated that the recoveries ranged between 99.0% and 102.2%, with an

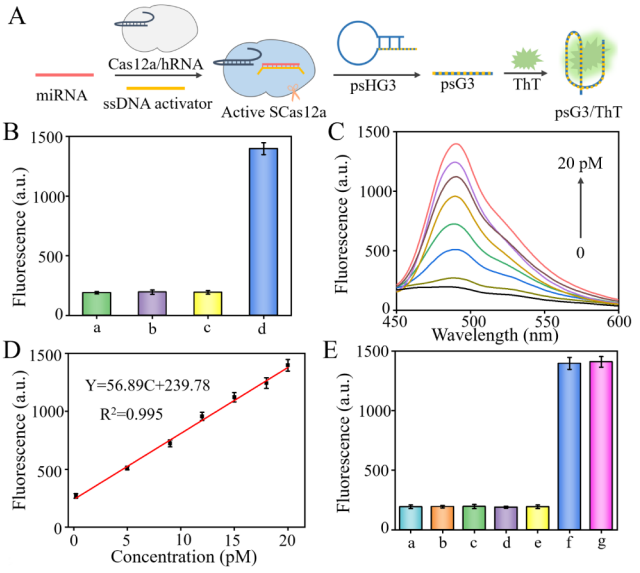


Figure 3. The SCas12a/psHG3 system used for detecting miRNA-21. (A) Schematic diagram of the SCas12a/psHG3 system for miRNA-21 detection. (B) Fluorescence intensity at 495 nm of the psG3 strategy in the presence of 20 pM miRNA-21. (a) psHG3 + ThT, (b) psHG3 + Cas12a + miRNA-21 + ssDNA + ThT, (c) psHG3 + Cas12a + hRNA + ssDNA + ThT, and (d) psHG + Cas12a + hRNA + ssDNA + miRNA-21 + ThT. (C) Fluorescence spectra of the SCas12a/psHG3 system for detection of 0, 0.2, 5, 9, 12, 15, 18, and 20 pM miRNA-21. (D) The linear plot of fluorescence intensity versus the concentration of miRNA-21 from 0.2 to 20 pM. (E) Selectivity of the SCas12a/psHG3 system for miRNA detection. (a) Blank, (b) miRNA-17, (c) miRNA-155, (d) miRNA-141, (e) miRNA-10b, (f) miRNA-21, and (g) mixture. Error bars: SD, n = 3.

RSD of less than 3.7%. Together, the results verified that the SCas12a/psHG3 system possesses the potential for clinical applications.

Sensing Performance of the SCas12a/psHG3 System for Kanamycin. Although the SCas12a/psHG3 system has achieved great success in nucleic acid detection, its application in non-nucleic acid detection still needs to be explored. Kanamycin is an aminoglycoside antibiotic derived from *Streptomyces kanamyceticus*, which is widely used in modern healthcare and food.[41,42] However, the misuse of kanamycin can cause excessive accumulation in the human body, causing antibiotic resistance and renal toxicity. Thus, the accurate detection of kanamycin is crucial for maintaining food safety and human health. Here, we chose kanamycin as the model target to evaluate the effectiveness of the SCas12a/psHG3 system for detecting non-nucleic acid targets. When kanamycin was added, it bonded to the AP sequence in the AP/CP complex and then released the CP sequence. Subsequently, the released CP sequence hybridized with the sRNA to activate the *trans*-cleavage activity of Cas12a, thereby initiating our signal-on fluorescence detection system (Figure 4A). As shown in Figure 4B, the SCas12a/psHG3 system was proven to be triggered only in the presence of kanamycin (30 nM) through the obtained fluorescence value, demonstrating its feasibility. By incubating the SCas12a/psHG3 system with increasing concentrations of kanamycin (0.3 to 30 nM), a corresponding increase in fluorescence values was observed (Figure 4C). Figure 4D shows that the fluorescence value was linearly correlated with the kanamycin concentration within the detection range of 0.3−30 nM, and the estimated LOD was

https://doi.org/10.1021/acs.analchem.5c00140
Anal. Chem. XXXX, XXX, XXX−XXX

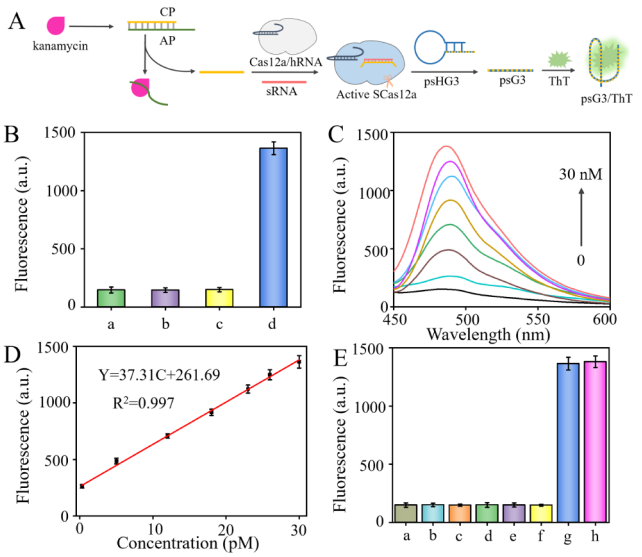


Figure 4. The SCas12a/psHG3 system used for kanamycin detection. (A) Schematic diagram of the SCas12a/psHG3 system for kanamycin detection. (B) Fluorescence intensity at 495 nm of the SCas12a/psHG3 system in the presence of 30 nM kanamycin. (a) psHG3 + ThT, (b) psHG3 + Cas12a + kanamycin + sRNA + AP/CP + ThT, (c) psHG3 + Cas12a + sRNA + hRNA + AP/CP + ThT, and (d) psHG3 + Cas12a + kanamycin + sRNA + hRNA + AP/CP + ThT. (C) Fluorescence spectra of the SCas12a/psHG3 system for detection of 0, 0.3, 5, 12, 18, 23, 26, and 30 nM kanamycin. (D) The linear plot of the fluorescence intensity versus the concentration of kanamycin from 0.3 to 30 nM. (E) Selectivity of the SCas12a/psHG3 system for kanamycin detection. (a) Blank, (b) tetracycline, (c) oxytetracycline, (d) ciprofloxacin, (e) ofloxacin, (f) sulfamerazine, (g) kanamycin, and (h) mixture. Error bars: SD, n = 3.

100 pM ($3\sigma/K$). The practical application value of detection methods relies not only on their sensitivity, but selectivity is also crucial. To explore the selectivity of the SCas12a/psHG3 system, six nontarget antibiotics, such as tetracycline, oxytetracycline, ciprofloxacin, ofloxacin, and sulfamerazine, were employed. Figure 4E shows that the SCas12a/psHG3 system achieved excellent selectivity for kanamycin detection since the blank control and other interfering antibiotics exhibited negligible fluorescence values. To verify that the psHG3/CRISPR strategy can be applied to aqueous solution samples, 5, 18, and 30 nM of kanamycin were added to tap water and river samples for analysis. Table S3 showed that satisfactory recoveries of 98.0% to 105.0% were obtained, and the RSD was below 5%. These results strongly suggest that the SCas12a/psHG3 system has potential in real sample applications.

CONCLUSIONS

In this study, we have systematically explored ps-modified G4 or G3 sequences that are not only tolerant to the *trans*-cleavage activity of CRISPR/Cas12a but also capable of binding to ThT in this system to produce fluorescence signals. By using reasonable sequence design, we have first reported a universal CRISPR/Cas12a-based "turn-on" fluorescent biosensor that utilizes the hairpin G3 as a reporter, known as SCas12a/psHG3. Using the SCas12a/psHG3 system, the nucleic acid and non-nucleic acid detection capabilities were demonstrated by modeling miRNA-21 and kanamycin targets, respectively. Under optimized conditions, the LOD values of miRNA-21 and kanamycin without preamplification were determined to be 100 fM and 100 pM, respectively. Furthermore, the SCas12a/psHG3 system has achieved sensitive, selective, and robust detection of miRNA-21 and kanamycin in human serum and environmental water samples. Nevertheless, the SCas12a/psHG3 system is limited to detecting a single target. Our future efforts will focus on improving the SCas12a/psHG3 system to enable the detection of multiple targets simultaneously in human serum and environmental water samples.

ASSOCIATED CONTENT

Supporting Information

The Supporting Information is available free of charge at https://pubs.acs.org/doi/10.1021/acs.analchem.5c00140.

Sequence information for the oligonucleotides, spiked recovery experiments of human serum and environmental water samples, melting curve of the psHG3 probe, and optimization of experimental conditions (PDF)

AUTHOR INFORMATION

Corresponding Authors

Kai Shi − *College of New Energy Materials and Chemistry, Leshan Normal University, Leshan, Sichuan 614000, P. R. China; Leshan West Silicon Materials Photovoltaic and New Energy Industry Technology Research Institute, Leshan, Sichuan 614000, P. R. China;* orcid.org/0000-0002-9181-5664; Email: shikai9901@163.com

Yu Hu − *College of New Energy Materials and Chemistry, Leshan Normal University, Leshan, Sichuan 614000, P. R. China; Leshan West Silicon Materials Photovoltaic and New Energy Industry Technology Research Institute, Leshan, Sichuan 614000, P. R. China*; Email: huyugucas@126.com

Jiaheng Zhang − *College of Chemistry, Zhengzhou University, Zhengzhou 450001, P. R. China;* orcid.org/0000-0002-8163-1706; Email: zhangjiaheng@zzu.edu.cn

Jiaxuan Chen − *College of New Energy Materials and Chemistry, Leshan Normal University, Leshan, Sichuan 614000, P. R. China; Leshan West Silicon Materials Photovoltaic and New Energy Industry Technology Research Institute, Leshan, Sichuan 614000, P. R. China;* Email: chenjx@lsnu.edu.cn

Authors

Wenjie Luo − *College of New Energy Materials and Chemistry, Leshan Normal University, Leshan, Sichuan 614000, P. R. China*

Ying Cheng − *College of New Energy Materials and Chemistry, Leshan Normal University, Leshan, Sichuan 614000, P. R. China*

Honglei Li − *College of New Energy Materials and Chemistry, Leshan Normal University, Leshan, Sichuan 614000, P. R. China*

Liai Peng − *College of New Energy Materials and Chemistry, Leshan Normal University, Leshan, Sichuan 614000, P. R. China*

Xiangrui Luo − *College of New Energy Materials and Chemistry, Leshan Normal University, Leshan, Sichuan 614000, P. R. China*

Complete contact information is available at: https://pubs.acs.org/10.1021/acs.analchem.5c00140

https://doi.org/10.1021/acs.analchem.5c00140
Anal. Chem. XXXX, XXX, XXX−XXX

Author Contributions

The manuscript was written with contributions from all authors.

Notes

The authors declare no competing financial interest.

■ ACKNOWLEDGMENTS

This work was supported by the National Natural Science Foundation of China (Nos. 22204066 and 22304165), the Sichuan Science and Technology Program (Nos. 2022JDRC0126 and MZGC20240115), the Leshan Science and Technology Bureau Program (Nos. 22CXY0003 and 24YYJC0030), and the Talents Scientific Research Launching Project of Leshan Normal University of China (No. RC2022002).

■ REFERENCES

(1) Jing, Z. W.; Li, R. F.; Zhao, J. W.; Yuan, R.; Chen, S. H. *Anal. Chem.* **2024**, *96* (45), 18178−18186.
(2) Chen, H.; Feng, Y.; Liu, F.; Tan, C. Y.; Xu, N. H.; Jiang, Y. Y.; Tan, Y. *Biosens. Bioelectron.* **2024**, *247*, 115929.
(3) Li, J. J.; Yang, S. S.; Zuo, C.; Dai, L.; Guo, Y. C.; Xie, G. M. *ACS Sens.* **2020**, *5* (4), 970−977.
(4) Li, D. X.; Liu, Y. H.; Li, Y. H.; Xiang, Y.; Yuan, R. *Anal. Chem.* **2024**, *96* (8), 3329−3334.
(5) Xu, J.; Liu, Y. B.; Huang, K.-J.; Wang, R. J.; Li, J. Q. *Chem. Eng. J.* **2023**, *466*, 143230.
(6) Li, D. X.; Gao, H. H.; Li, Y. H.; Yuan, R.; Xiang, Y. *Food Control* **2025**, *169*, 111007.
(7) He, Y. Q.; Chen, Y.; Meng, X. Z.; Yi, H. C.; Gu, H. W.; Yin, H. L. *Sens. Actuators, B* **2023**, *376*, 132976.
(8) Iglói, Z.; leven, M.; Abou-Nouar, Z. A.-K.; Weller, B.; Matheeussen, V.; Coppens, J.; Koopmans, M.; Molenkamp, R. *J. Clin. Virol.* **2020**, *129*, 104510.
(9) Shalaby, A. A.; Maeda, R.; Ishida, A.; Shimizu, Y.; Saeki, H.; Maeki, M.; Tokeshi, M. *Sens. Actuators, B* **2025**, *422*, 136536.
(10) Pilli, S.; Pandey, A. K.; Pandey, V.; Pandey, K.; Muddam, T.; Thirunagari, B. K.; Thota, S. T.; Varjani, S.; Tyagi, R. D. J. *J. Environ. Manage.* **2021**, *297*, 113336.
(11) Ozdemir, A.; Lin, J.-L.; Gulfen, M.; Chen, C.-H. *Talanta* **2024**, *273*, 125929.
(12) Gong, S.; Song, K.; Pan, W.; Li, N.; Tang, B. *Anal. Chem.* **2024**, *96* (39), 15789−15796.
(13) Meng, X.; Gu, H.; Yin, X.; Yi, H.; Chen, Y. *Chem. Commun.* **2023**, *59* (51), 7939−7942.
(14) Doudna, J. A.; Charpentier, E. *Science* **2014**, *346* (6213), 1258096.
(15) Pickar-Oliver, A. P.; Gersbach, C. A. *Nat. Rev. Mol. Cell Biol.* **2019**, *20* (8), 490−507.
(16) Gootenberg, J. S.; Abudayyeh, O. O.; Lee, J. W. *Science* **2017**, *356* (6336), 438−442.
(17) Chen, J. S.; Ma, E.; Harrington, L. B.; Da Costa, M.; Tian, X.; Palefsky, J. M.; Doudna, J. A. *Science* **2018**, *360*, 436−439.
(18) Li, S. Y.; Cheng, Q. X.; Liu, J. K.; Nie, X. Q.; Zhao, G. P.; Wang, J. *Cell Res.* **2018**, *28*, 491−493.
(19) Kaminski, M. M.; Abudayyeh, O. O.; Gootenberg, J. S.; Zhang, F.; Collins, J. J. *Nat. Biomed. Eng.* **2021**, *5*, 643−656.
(20) Li, H. M.; Xie, Y.; Chen, F. M.; Bai, H. W.; Xiu, L. S.; Zhou, X. N.; Guo, X. K.; Hu, Q. Q.; Yin, K. *Chem. Soc. Rev.* **2023**, *52*, 361−382.
(21) Phan, Q. A.; Truong, L. B.; Medina-Cruz, D.; Dincer, C.; Mostafavi, E. *Biosens. Bioelectron.* **2022**, *197* (197), 113732.
(22) Zeng, J.; Liu, P.; Du, J.; Li, S.; Xiong, E.; Yang, R. *Sci. China: Chem.* **2024**, *68* (2), 789−801.
(23) Chen, Y.; Wang, X.; Zhang, J.; Jiang, Q.; Qiao, B.; He, B.; Yin, W.; Qiao, J.; Liu, Y. *Nat. Commun.* **2024**, *15* (1), 8342.
(24) Shi, K.; Xie, S.; Tian, R.; Wang, S.; Lu, Q.; Gao, D.; Lei, C.; Zhu, H.; Nie, Z. *Sci. Adv.* **2021**, *7* (5), No. eabc7802.
(25) Dai, Y.; Somoza, R. A.; Wang, L.; Welter, J. F.; Li, Y.; Caplan, A. I.; Liu, C. C. *Angew. Chem., Int. Ed.* **2019**, *131* (48), 17560−17566.
(26) Gong, S.; Zhang, S.; Wang, X.; Li, J.; Pan, W.; Li, N.; Tang, B. *Anal. Chem.* **2021**, *93* (45), 15216−15223.
(27) Zhao, Y.; Chen, D.; Xu, Z.; Li, T.; Zhu, J.; Hu, R.; Xu, G.; Li, Y.; Yang, Y.; Liu, M. *Anal. Chem.* **2023**, *95* (6), 3476−3485.
(28) Peng, S.; Tan, Z.; Chen, S. Y.; Lei, C. Y.; Nie, Z. *Chem. Sci.* **2020**, *11* (28), 7362−7368.
(29) Zhao, X. H.; Zhou, Y. N.; Lv, X. Z.; Zhang, H. X.; Cui, X. H.; Gong, T.; Meng, H. M.; Yin, L. T.; Li, G. P.; Yu, B. F. *Sens. Actuators, B* **2023**, *380*, 133310.
(30) Zhang, D. C.; Tian, B. S.; Ling, Y.; Ye, L.; Xiao, M.; Yuan, K. X.; Zhang, X. Q.; Zheng, G. S.; Li, X. Y.; Zheng, J. D.; Liao, Y. H.; Shu, B. W.; Gu, B. *Anal. Chem.* **2024**, *96* (25), 10451−10458.
(31) Huang, R.; Li, M.; Qu, Z.; Liu, Y.; Lu, X.; Li, R.; Zou, L. *Food Res. Int.* **2024**, *180*, 114058.
(32) Li, T.; Hu, R.; Xia, J. B.; Xu, Z. C.; Chen, D. G.; Xi, J. O.; Liu, B.-F.; Zhu, J.; Li, Y.; Yang, Y. H.; Liu, M. L. *Biosens. Bioelectron.* **2021**, *187*, 113292.
(33) Chen, X. Y.; Wang, L.; He, F.; Chen, G. H.; Bai, L. L.; He, K. Y.; Zhang, F.; Xu, X. H. *Anal. Chem.* **2021**, *93* (42), 14300−14306.
(34) Wu, Y.; Lai, R. Y. *Anal. Chem.* **2017**, *89* (18), 9984−9989.
(35) Ding, H.; Zhang, M.; Wang, X.; He, S.; Wang, X.; Chen, L. *Anal. Chim. Acta* **2024**, *1299*, 342440.
(36) Shi, K.; Tian, Y.; Liu, S. J.; Luo, W. J.; Liu, K. E.; Zhang, L.; Zhang, Y.; Chang, J. L.; Zhang, J. H.; Wang, S. *Anal. Chim. Acta* **2024**, *1308*, 342649.
(37) Zhou, Y. M.; Xie, S.; Liu, B.; Wang, C.; Huang, Y. B.; Zhang, X. R.; Zhang, S. *Anal. Chem.* **2023**, *89*, 3332−3339.
(38) Liu, H.; Dong, J.; Duan, Z.; Xia, F.; Willner, I.; Huang, F. *Sci. Adv.* **2024**, *10* (30), No. eadp6166.
(39) Yang, L. M.; Guo, H.; Gao, Q.; Hou, T.; Zhang, J. G.; Liu, X. J.; Li, F. *Anal. Chem.* **2023**, *95* (48), 17834−17842.
(40) Wu, J. H.; Lv, W. X.; Yang, Q. T.; Li, H. Y.; Li, F. *Biosens. Bioelectron.* **2021**, *171*, 112707.
(41) Ye, T.; Lu, J. Q.; Yuan, M.; Cao, H.; Yin, F. Q.; Wu, X. X.; Hao, L. L.; Xu, F. *Sens. Actuators, B* **2021**, *340*, 129939.
(42) Hu, J. Y.; Song, H. J.; Zhou, J.; Liu, R.; Lv, Y. *Anal. Chem.* **2021**, *93* (42), 14214−14222.

https://doi.org/10.1021/acs.analchem.5c00140
Anal. Chem. XXXX, XXX, XXX−XXX